U.S. DEPARTMENT OF COMMERCE
National Oceanic and Atmospheric Administration
Environmental Research Laboratories

NOAA Technical Memorandum ERL NSSL-60

SIMULATED REAL-TIME DISPLAYS OF DOPPLER RADAR VELOCITY FIELDS

G. B. Walker
National Severe Storms Laboratory

L. D. Hennington
Oklahoma University Research Institute

Property of
NWC Library
University of Oklahoma

National Severe Storms Laboratory
Norman, Oklahoma
November 1972

TABLE OF CONTENTS

	Page
LIST OF FIGURES	v
ABSTRACT	1
1. INTRODUCTION	1
2. SIMULATION STUDY	2
3. CONCLUSIONS	3
4. APPENDIX	9

LIST OF FIGURES

Figure		Page
1.	Contoured echo intensity display of squall line as seen by NSSL's WSR-57 radar, 2021 CST, 2 June 1971. Elevation angle is 1°. Outlined area is region of Doppler velocity measurements. Intensity Scale: $\log_{10}Z$ = 1-2,2-3,3-4,4-5, 5-6 corresponds to gray, white, black, gray, white, respectively.	4
2.	Display of mean velocity versus radar range and azimuth. Trace vertical displacement is proportional to mean velocity for each volume sample. Sample spacing and size in range are 600 meters and 150 meters, respectively. Horizontal straight lines are zero velocity references for each range sample. The velocity scale is approximately 35 m sec^{-1} between zero reference lines.	4
3.	Display of mean velocity versus radar range and azimuth. Same as figure 2 without the zero velocity references.	5
4.	Display of mean and standard deviation versus radar and azimuth. Same as figure 2 except the vertical width of each trace is proportional to the standard deviation of the velocity spectrum in each volume sample.	5
5.	Display of mean and velocity standard deviation versus radar range and azimuth. Same as figure 4 without the zero velocity references.	6
6.	Comparison of velocity displays with and without fold/image check in computer processing of data.	6
7.	Alphanumeric display of mean velocity. A symbol is printed for each sample volume. Hyphens are where echoes were not detected, and blanks correspond to velocity intervals between those indicated in the scale above. Velocity intervals 2.5 m sec^{-1}.	7
8.	Alphanumeric display. Same as figure 7 except velocity intervals set at 5 m sec^{-1}.	7
9.	Alphanumeric display. Same as figure 7 except velocity intervals set at 10 m sec^{-1}.	8
10.	Alphanumeric display. Same as figure 7 except velocity intervals set at 20 m sec^{-1}.	9
A1.	Flow diagram of Doppler radar velocity program.	10

SIMULATED REAL-TIME DISPLAYS OF DOPPLER RADAR VELOCITY FIELDS

G. B. Walker
National Severe Storms Laboratory

L. D. Hennington
Oklahoma University Research Institute

ABSTRACT

This report describes a technique to display, in real time, severe storm velocities available from a Doppler radar. Velocity combined with storm precipitation intensity on a PPI and/or a RHI display offers the Doppler radar operator information to determine if a storm is suitable for detailed investigation and data to establish range, azimuth, and elevation limits necessary to sample the storm. We used a digital computer and a storage oscilloscope display to process Doppler velocity data taken from a squall line on 2 June 1971 with NSSL's 10-cm Doppler radar. Mean Doppler radial velocity is presented as vertical displacements for each volume, sampled as a function of range and azimuth. Standard deviation is shown as broadening of the mean velocity trace. Regions of high shear and turbulence are clearly visible. A second technique presents mean Doppler velocity as an alphanumeric display for velocity intervals ranging from 2.5 m sec^{-1} to 20 m sec^{-1}. Composites of eight photographs of the storage display cover the storm section. Computation time for 64 range locations was 20 m sec, whereas radar dwell time is about 250 m sec, indicating a real-time capability.

1. INTRODUCTION

The National Severe Storms Laboratory, aiming to advance knowledge of severe storm morphology and dynamics, has established a Doppler radar system to determine air flow. Velocity information combined with storm precipitation intensity displayed on a PPI scope and/or a RHI scope offers the Doppler system operator information both to determine storm suitability for detailed study and to establish azimuth, elevation, and range limits required to sample the storm.

This study tests the feasibility and practicality of displaying spectral moments of actual storm data in alphanumeric or graphic forms on CRT displays. The data inputs for the simulation originated from a squall line that formed in southern Kansas, during the afternoon of 2 June 1971, and moved south-southeast through central Oklahoma. Time series data, the Quadrature and Inphase components available as Doppler radar outputs, were collected at Norman, Oklahoma from this squall line with a modified FPS-18 radar (NSSL's 10-cm Doppler radar: WDS-71). Mean and standard deviation of the velocity spectrum are computed from these data by using Fast Fourier analysis, and these results, as well as housekeeping parameters (e.g., range, time, angle etc.) are then stored on magnetic tape and are the data inputs required for

simulation of the real-time display.

2. SIMULATION STUDY

The simulated real-time displays were provided by the Doppler Radar Velocity Program (DRVP) developed as a part of this study. The DRVP aids in evaluating prospects of real-time analysis and graphic display of severe storm velocity information available from a Doppler radar and velocity processor. The DRVP comprises a series of sub-programs to generate graphic or alphanumeric displays for evaluation. These programs were designed and executed by a PDP-9/L computer and a Tektronic 611 storage display[1]. The programming was in machine language using the PDP-9/L assembler and ODT-9 (octal debugging technique). A simplified flow diagram used in the DRVP is given in the appendix.

The storm segment selected for study was 74 km to 112 km from the radar at an azimuth of 310° to 350° (see figure 1). Figure 1 presents NSSL's WSR-57 radar contoured echoes from the 2 June 1971 squall line. The Doppler velocity data were taken from the region outlined in white. Sixty-four range samples were taken at an elevation angle of 1° and at 0.5° azimuth intervals. These data are shown in figures 2 through 6; alphanumerical data are in figures 7 through 10. Figure 2 shows mean Doppler radial velocity versus radar range and azimuth. Each graphic display trace radial records precipitation particle velocities along a circumferential arc at a fixed range. Vertical displacement of each trace is proportional to the mean velocity for the volume sample, and the sample range spacing is 600 meters. Volume sampled is assumed to be the antenna beam cross sectional area (at the 3 dB width) in meter^2, at a given range, times 150 meters (150 meters corresponds to the time-sample window coverted to space). The horizontal straight lines are zero velocity references located at each range sampled. The distance between zero reference lines represents $\pm$ 35.8 m sec^{-1}. Regions of shear wind are (clearly visible) near the graph's center. All the graphic displays, except figure 6, are a composite of eight photographs taken from the Tektronix 611 storage display.

Figure 3 removes the zero velocity reference lines in figure 2. The blank areas evident in figures 2 and 3 are regions without data, (insufficient radar return for Doppler measurements).

Figure 4 incorporates the velocity standard deviation (second moment about mean) that is porportional to the vertical width of the velocity trace. The mean displacement of the line is proportional to the mean velocity. Figure 5 is again figure 4 without the zero reference lines.

---

[1]The PDP-9/L high speed computer, at the University of Oklahoma College of Engineering, is a single address, parallel binary computer with 8K of addressable memory and a cycle time of 1.5 microseconds. The Tektronix 611 storage employs a storage oscilloscope with 4096 by 4096 addressable points. Mention of commercial products does not imply endorsement.

There is a maximum unambiguous velocity measurable by a Doppler radar with fixed parameters. For the NSSL radar, which uses a pulse repetition frequency of 1300 and a wavelength of 10.6 cm, the maximum unambiguous velocity is $\pm$ 34.5 m sec^{-1}. When the velocity of the scatterers exceeds this maximum, the velocity spectrum folds, which can lead to calculated estimates many times greater than the actual velocity spectrum standard deviation. NSSL has developed a computer technique to automatically detect and correct the folding for many cases. Figure 6 contrasts "raw" velocity data display and one generated after correcting the folds. These data were taken from a high velocity region of a severe storm on 31 May 1971.

Alphanumeric displays of Doppler velocity information for the 2 June 1971 storm are shown in figures 7 through 10. These were generated with the Tektronix 611 character generating routine. The display shows just the velocity at a particular sample volume. Here, numbers correspond to negative velocities and letters are positive velocities (away from the radar). Zero indicates velocities near zero and dashes mean "no data." Characters indicate velocity intervals and not the specific velocities. The velocity intervals indicated by characters are separated by blanks (absence of characters), which represent velocity intervals between the characterized ones. Figures 7 through 10 are presentations with sequentially decreasing resolution of velocity details.

3. CONCLUSIONS

The experimental alphanumeric and graphic displays illustrated here simulate displays obtainable under real-time conditions. The real-time capabilities are evident from comparison of present Doppler radar data collection time per radial (dwell times = 250 m sec) with the PDP-9/L and Tektronix 611 computational and display time (20 m sec for 64 range locations). Actual times for each display are formulated in the appendix.

As our interpretive abilities improve, we (may) expect real-time displays such as presented here to become valuable aids in operational use of Doppler radar for storm warning and aviation forecasting. Early use of such displays should, in research settings, contribute to understanding of Doppler radar applications.

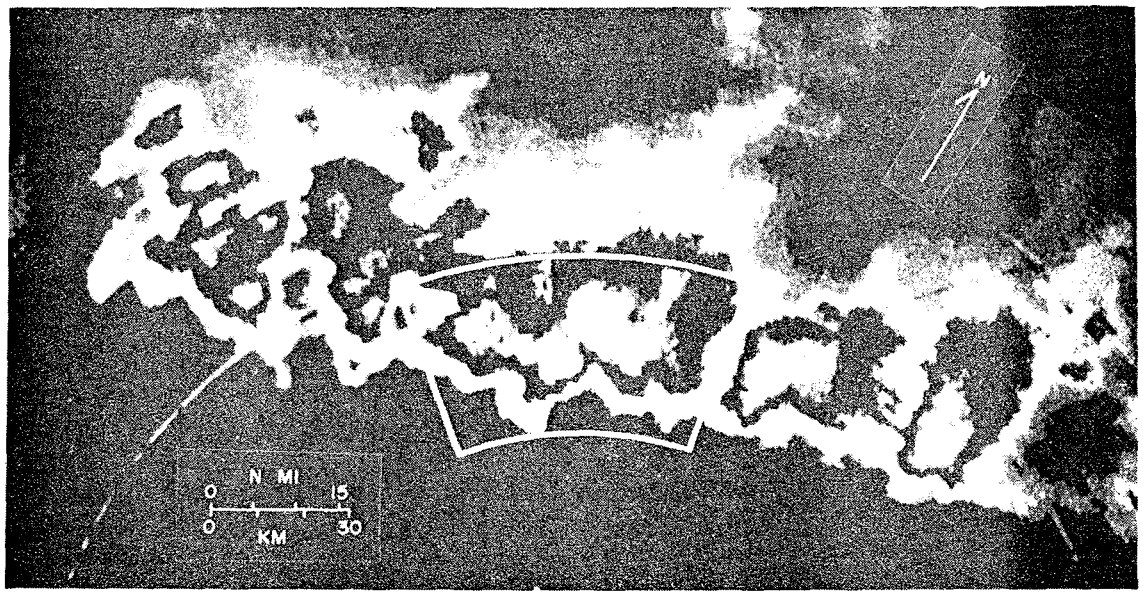

Figure 1. Contoured echo intensity display of squall line as seen by NSSL's WSR-57 radar, 2021 CST, 2 June 1971. Elevation angle is 1°. Outlined area is region of Doppler velocity measurements. Intensity Scale: $\log_{10}Z$ = 1-2,2-3,3-4,4-5,5-6 corresponds to gray, white, black, gray, white, respectively.

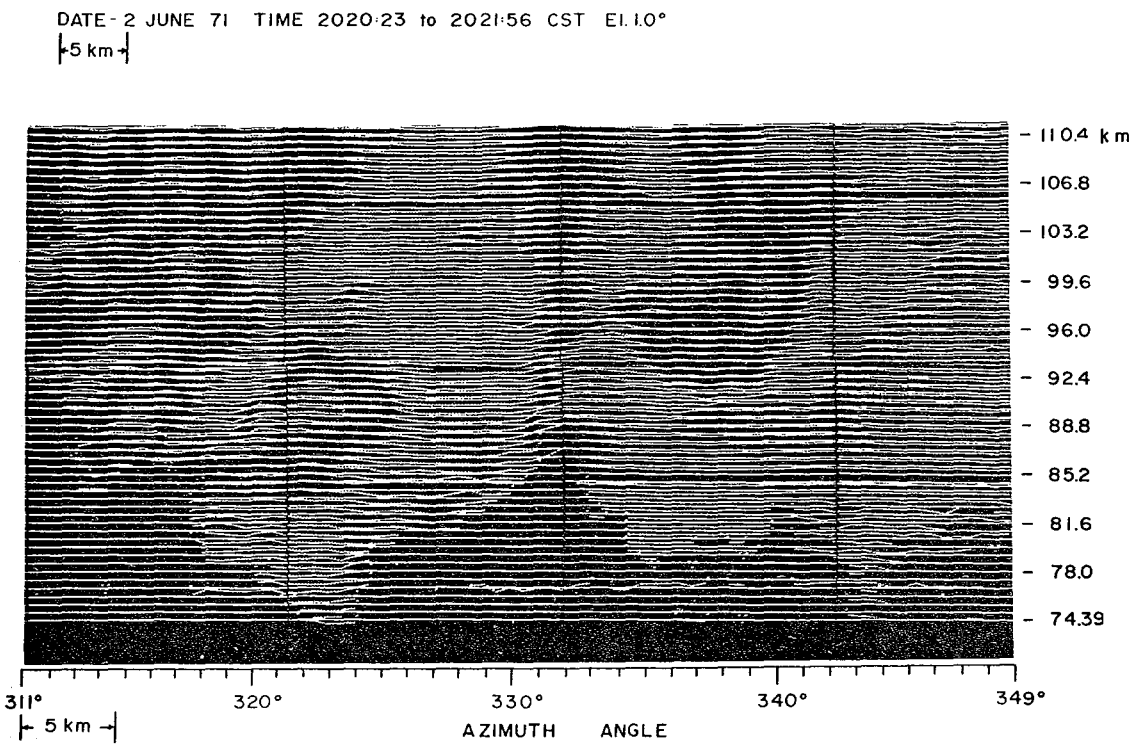

Figure 2. Display of mean velocity versus radar range and azimuth. Trace vertical displacement is proportional to mean velocity for each volume sample. Sample spacing and size in range are 600 meters and 150 meters, respectively. Horizontal straight lines are zero velocity references for each range sample. The velocity scale is approximately 35 m sec^{-1} between zero reference lines.

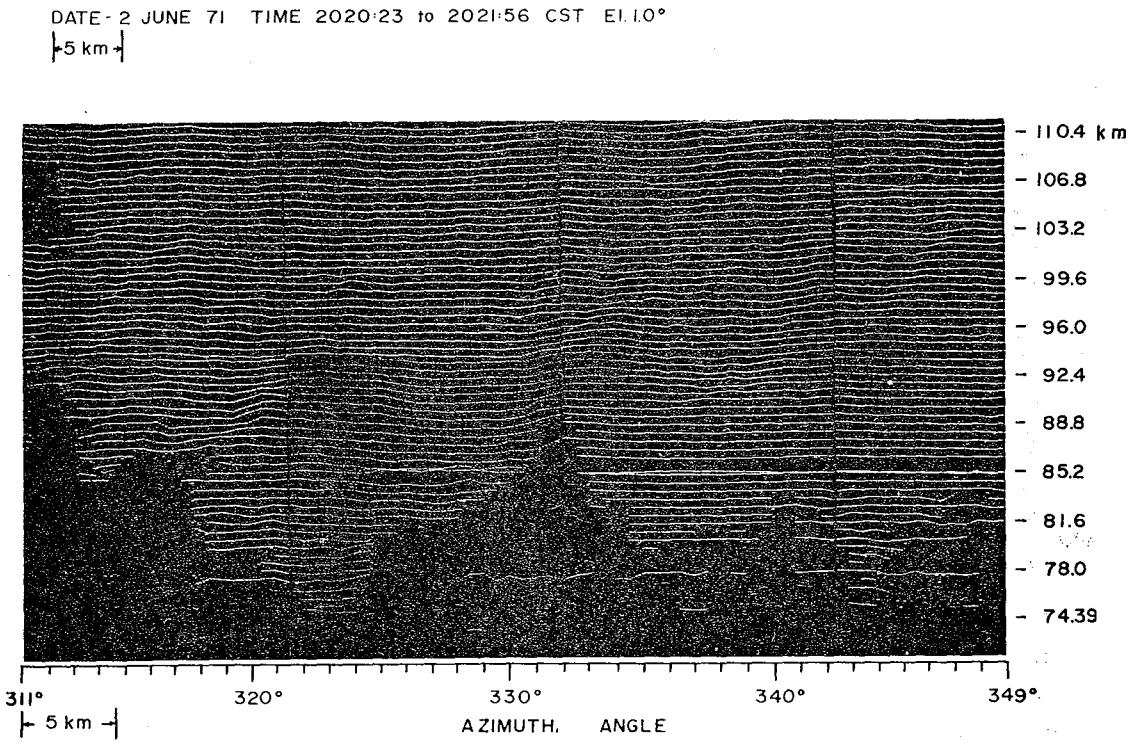

Figure 3. Display of mean velocity versus radar range and azimuth. Same as figure 2 without the zero velocity references.

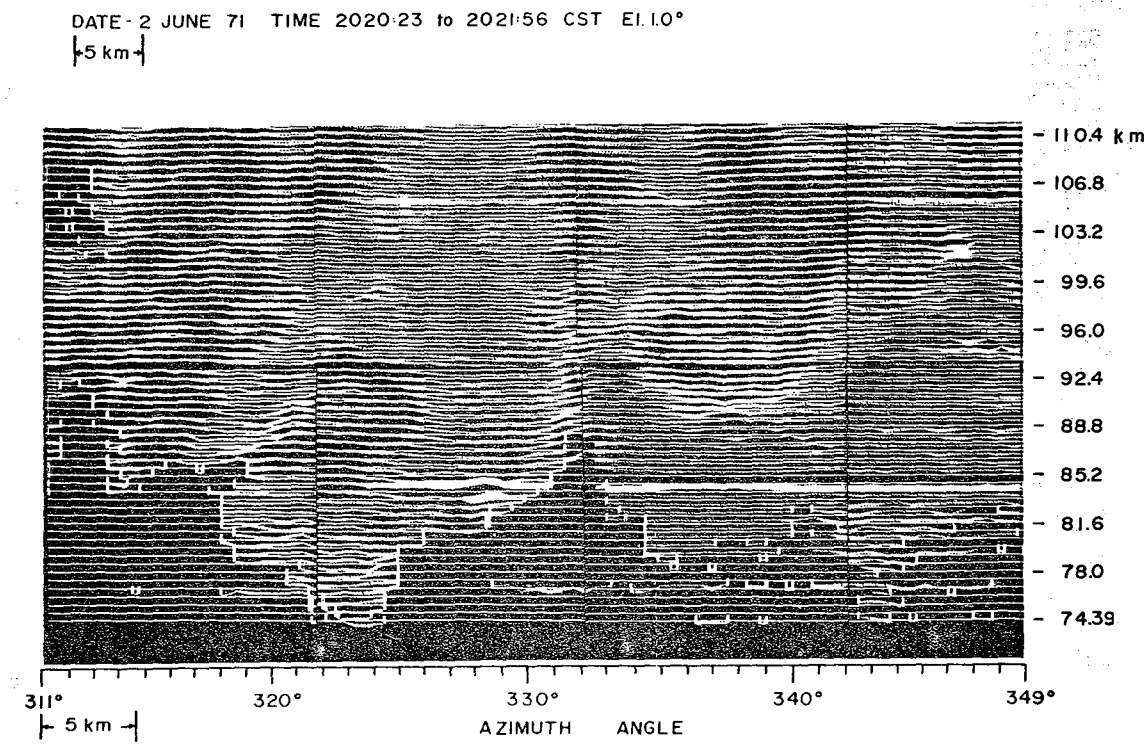

Figure 4. Display of mean and standard deviation versus radar range and azimuth. Same as figure 2 except the vertical width of each trace is proportional to the standard deviation of the velocity spectrum in each volume sample.

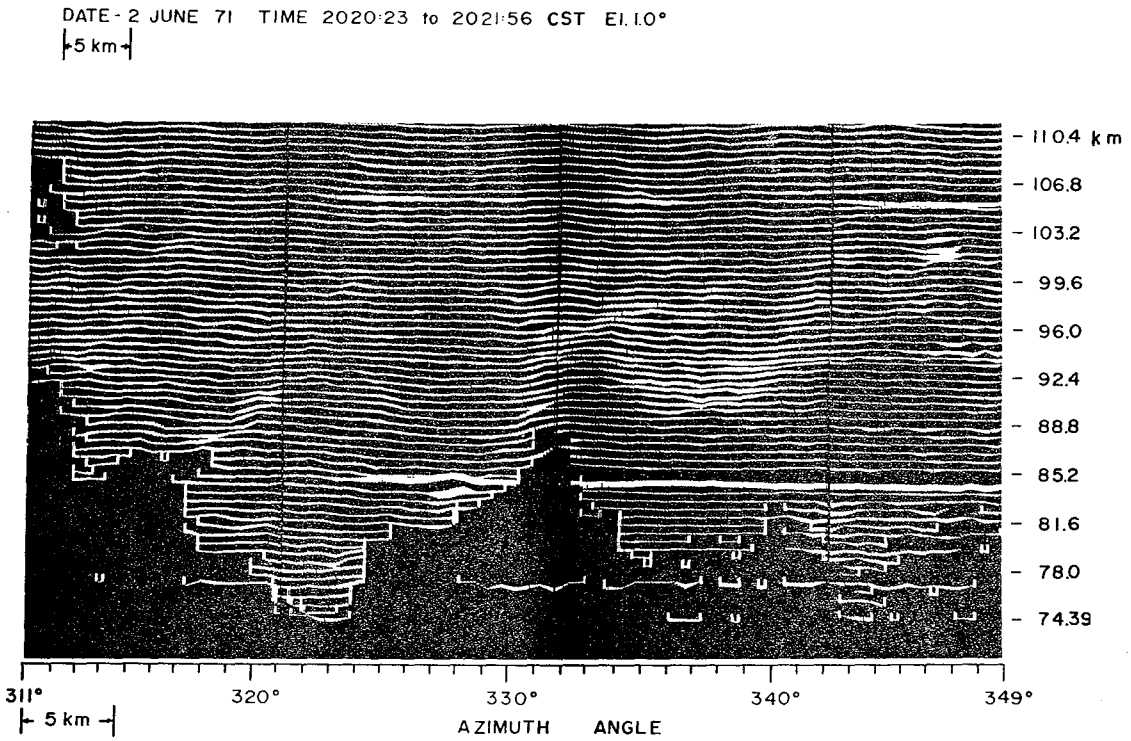

Figure 5. Display of mean and velocity standard deviation versus radar range and azimuth. Same as figure 4 without the zero velocity references.

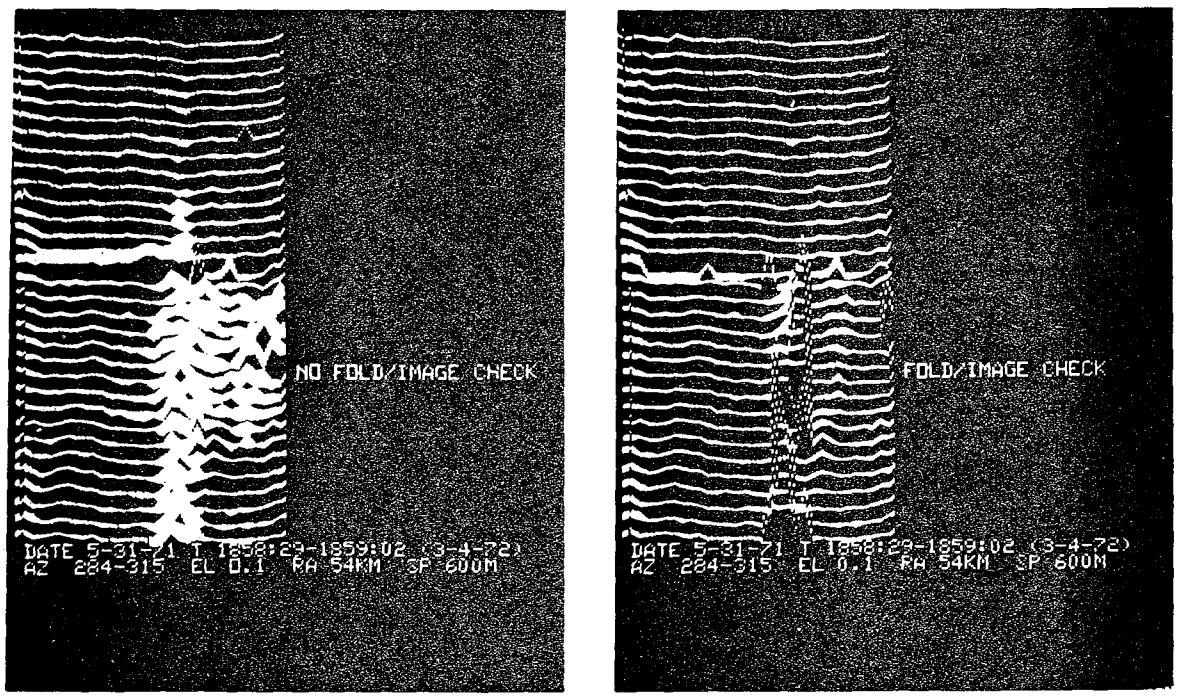

Figure 6. Comparison of velocity displays with and without fold/image check in computer processing of data.

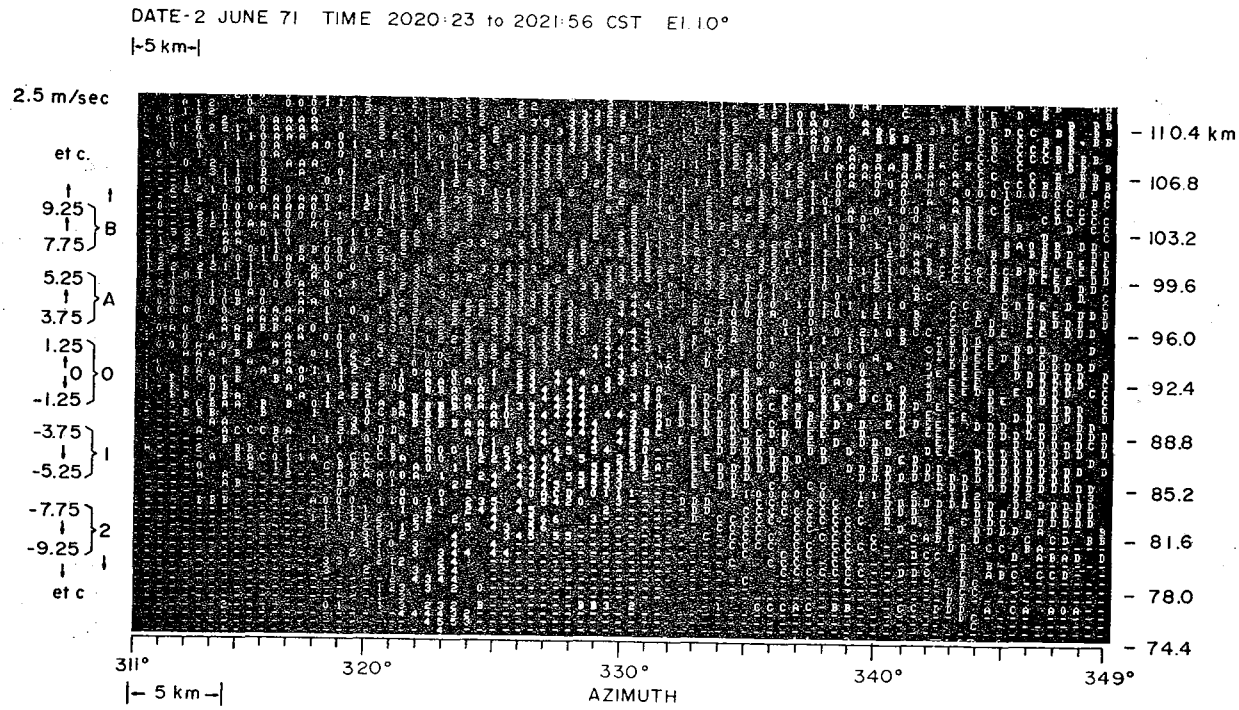

Figure 7. Alphanumeric display of mean velocity. A symbol is printed for each sample volume. Hyphens are where echoes were not detected, and blanks correspond to velocity intervals between those indicated in the scale above. Velocity intervals 2.5 m sec^{-1}.

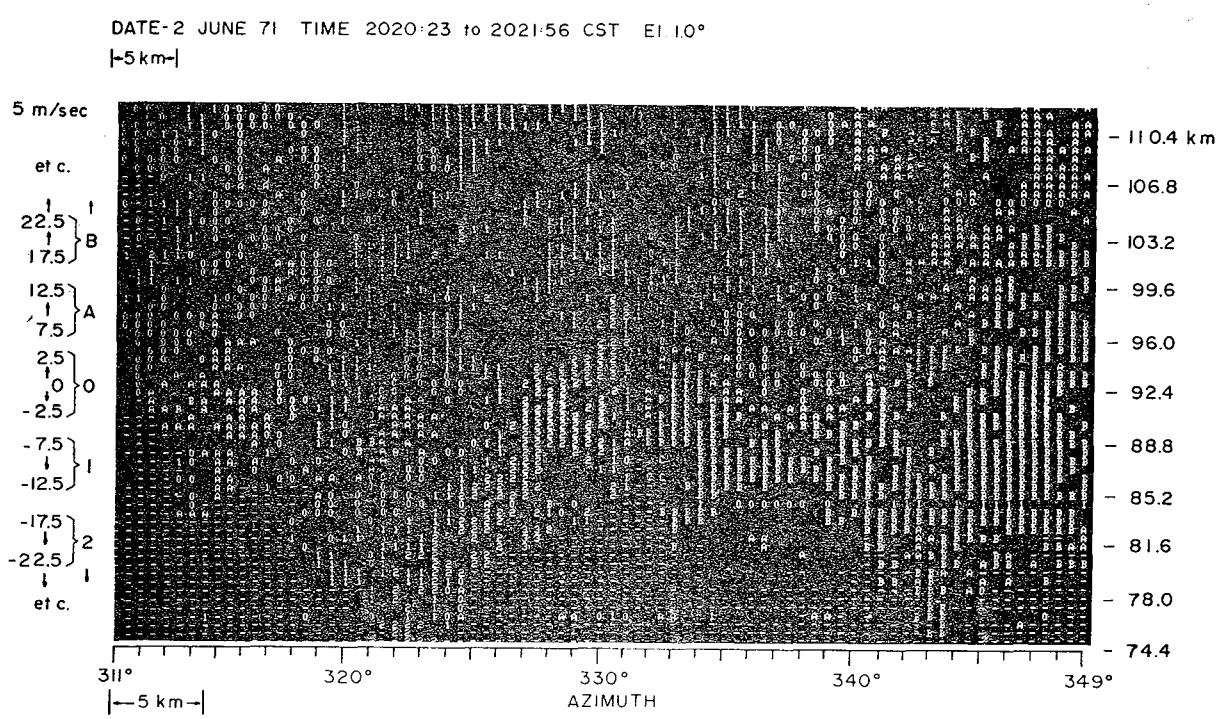

Figure 8. Alphanumeric display. Same as figure 7 except velocity intervals set at 5 m sec^{-1}.

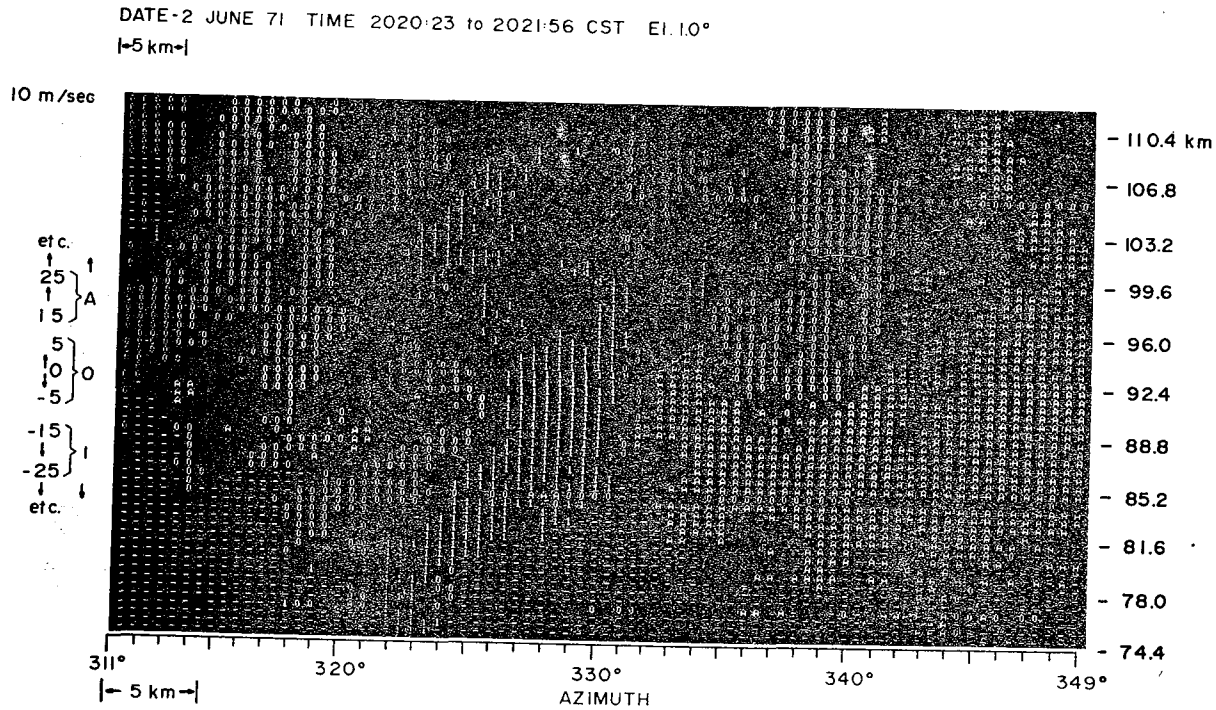

Figure 9. Alphanumeric display. Same as figure 7 except velocity intervals set at 10 m sec^{-1}.

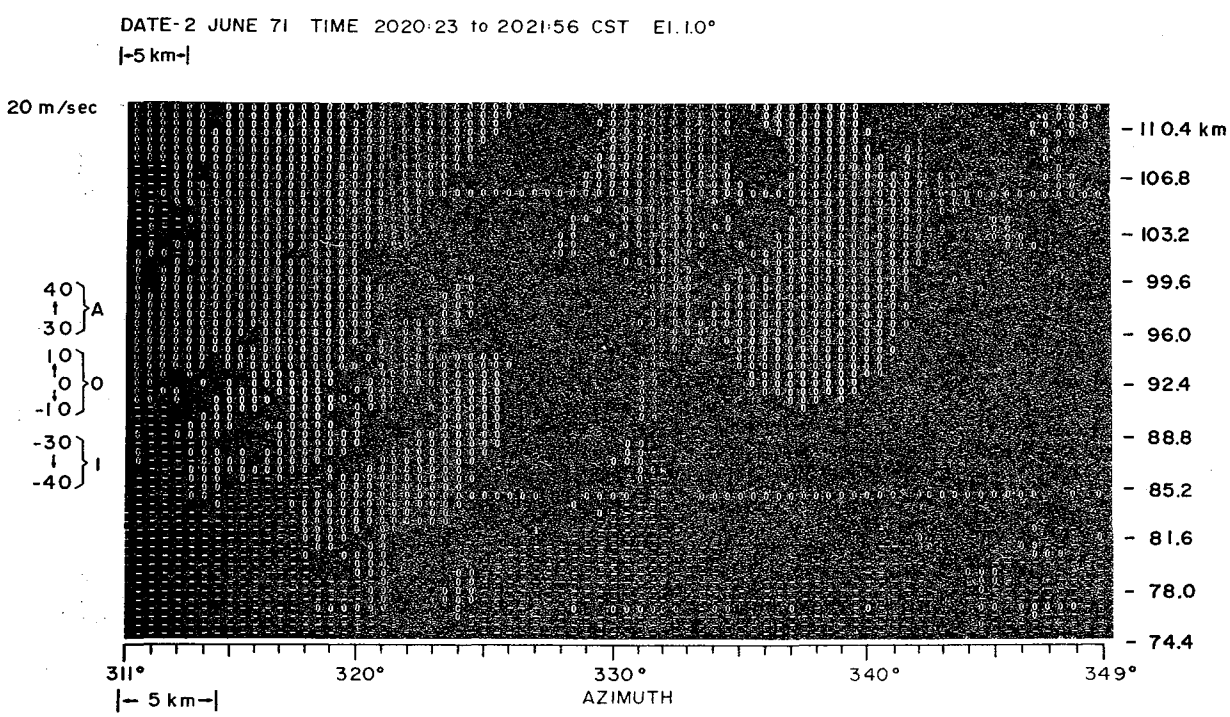

Figure 10. Alphanumeric display. Same as figure 7 except velocity intervals set at 20 m sec^{-1}.

APPENDIX

Flow Diagram of Doppler Radar Velocity Program

During data processing, three interpolated points are generated between each pair of data points to give continuity to the generated graphical curves. Arrays of numbers are then generated for velocity and standard deviation. In the flow diagram, figure A1, V(I,J) is the velocity for azimuth 'I' and range gate 'J', and σ (I,J) is the corresponding standard deviation; X and Y are the coordinates on the oscilloscope; and Δ AZ is the distance on the scope between azimuths. Distance on the scope refers to the number of addressable points between two locations. The distance between two adjacent addressable points represents, for the case used in this simulation, a velocity scale of 0.23 m sec^{-1} and a range scale of 3.8 meters. The term ΔR equals the distance on the scope between gates; IMAX is the total number of azimuthal locations; and JMAX is the total number of Doppler radar sampled range locations.

The flow diagram is for the graph routine; however, the alphanumeric routine (except instead of drawing a line) evaluates the velocity and draws its representative character. The standard deviation was not programmed for alphanumeric displays.

Time Required for Displays

The following equation determines the time required to draw a complete graphical display of spectrum mean and standard deviation on the Tektronix 611:

$$[\mathrm{Jmax}\ (\Delta R\ (\mathrm{DPT}) + \mathrm{DST})]\mathrm{IMAX} + (\Delta AZ\ (\mathrm{DPT}) + \mathrm{DST})\mathrm{Imax}$$

$$+ (\mathrm{DWT})\ \left(\sum_{I=1}^{\mathrm{Imax}} \sum_{J=1}^{\mathrm{Jmax}} \sigma(I,J)\right)/0.23 = T.$$

Where T = time for one graph display in seconds, DWT = dot writing time = 20 μ sec, DPT = dot positioning time (between contiguous addressable locations) = 14 nsec, and DST = dot settling time = 5 μ sec. For the figure 2 example, where IMAX = 618, JMAX = 64, and σ (I,J) = 1 (1 is the smallest length that can be drawn), the time required is 3.73 sec.

To find the time for an alphanumeric display using the equation above, replace

$$\sum_{I=1}^{\mathrm{IMAX}} \sum_{J=1}^{\mathrm{JMAX}} (I,J)/0.23$$

with the number of characters to be drawn times the number of dots per character. (Average character consists of 20 dots.)

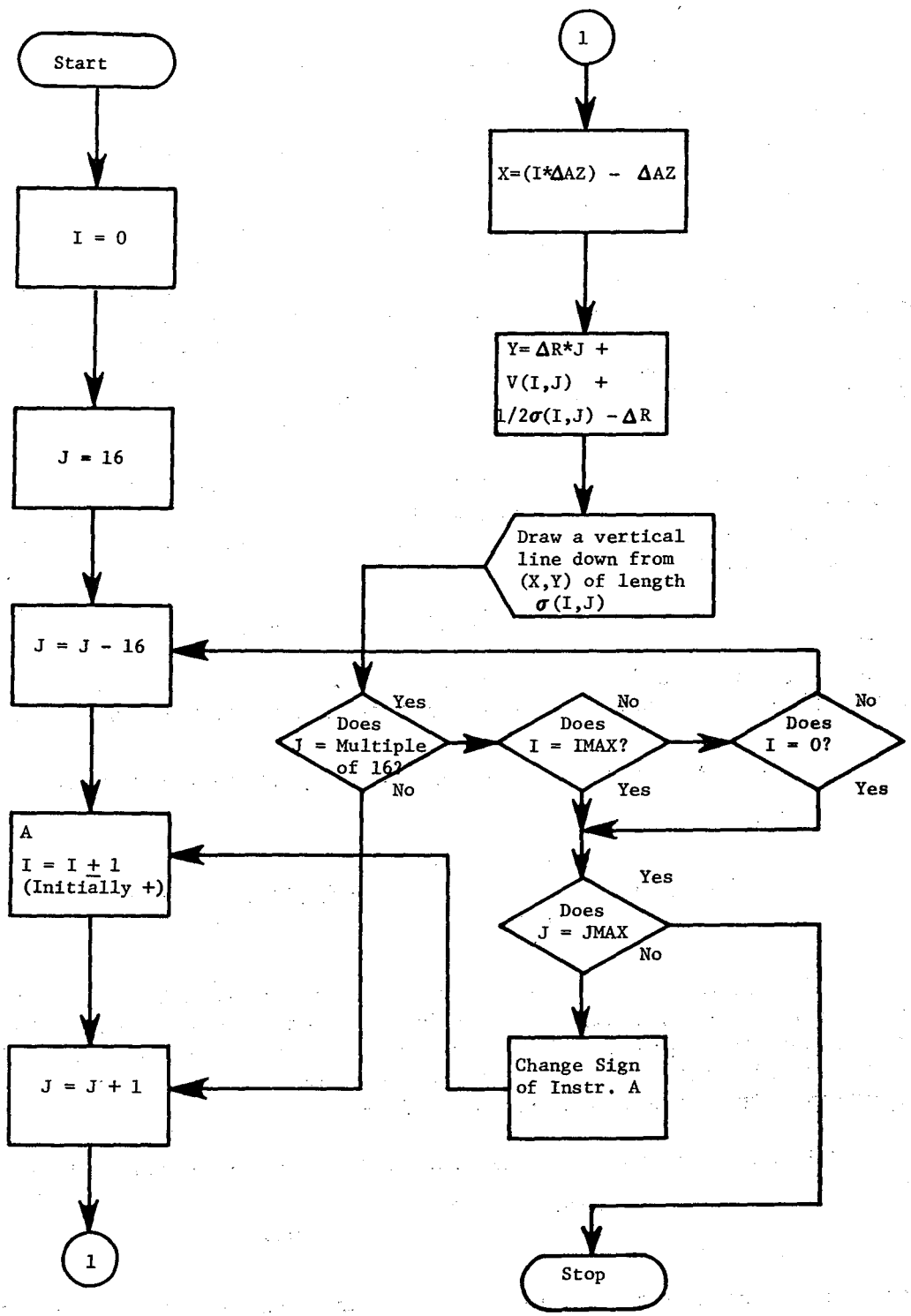

Figure A1. Flow diagram of Doppler radar velocity program.

NATIONAL SEVERE STORMS LABORATORY

The NSSL Technical Memoranda, beginning with No. 28, continue the sequence established by the U. S. Weather Bureau National Severe Storms Project, Kansas City, Missouri. Numbers 1-22 were designated NSSP Reports. Numbers 23-27 were NSSL Reports, and 24-27 appeared as subseries of Weather Bureau Technical Notes. These reports are available from the National Technical Information Service, Operations Division, Springfield, Virginia 22151, for $3.00, and a microfiche version for $0.95. NTIS numbers are given below in parentheses.

No. 1 National Severe Storms Project Objectives and Basic Design. Staff, NSSP. March 1961. (PB-168207)

No. 2 The Development of Aircraft Investigations of Squall Lines from 1956-1960. B. B. Goddard. (PB-168208)

No. 3 Instability Lines and Their Environments as Shown by Aircraft Soundings and Quasi-Horizontal Traverses. D. T. Williams. February 1962. (PB-168209)

No. 4 On the Mechanics of the Tornado. J. R. Fulks. February 1962. (PB-168210)

No. 5 A Summary of Field Operations and Data Collection by the National Severe Storms Project in Spring 1961. J. T. Lee. March 1962. (PB-165095)

No. 6 Index to the NSSP Surface Network. T. Fujita. April 1962. (PB-168212)

No. 7 The Vertical Structure of Three Dry Lines as Revealed by Aircraft Traverses. E. L. McGuire. April 1962. (PB-168213)

No. 8 Radar Observations of a Tornado Thunderstorm in Vertical Section. Ralph J. Donaldson, Jr. April 1962. (PB-174859)

No. 9 Dynamics of Severe Convective Storms. Chester W. Newton. July 1962. (PB-163319)

No. 10 Some Measured Characteristics of Severe Storms Turbulence. Roy Steiner and Richard H. Rhyne. July 1962. (N62-16401)

No. 11 A Study of the Kinematic Properties of Certain Small-Scale Systems. D. T. Williams. October 1962. (PB-168216)

No. 12 Analysis of the Severe Weather Factor in Automatic Control of Air Route Traffic. W. Boynton Beckwith. December 1962. (PB-168217)

No. 13 500-Kc./Sec. Sferics Studies in Severe Storms. Douglas A. Kohl and John E. Miller. April 1963. (PB-168218)

No. 14 Field Operations of the National Severe Storms Project in Spring 1962. L. D. Sanders. May 1963. (PB-168219)

No. 15 Penetrations of Thunderstorms by an Aircraft Flying at Supersonic Speeds. G. P. Roys. Radar Photographs and Gust Loads in Three Storms of 1961 Rough Rider. Paul W. J. Schumacher. May 1963. (PB-168220)

No. 16 Analysis of Selected Aircraft Data from NSSP Operations, 1962. T. Fujita. May 1963. (PB-168221)

No. 17 Analysis of Methods for Small-Scale Surface Network Data. D. T. Williams. August 1963. (PB-168222)

No. 18 The Thunderstorm Wake of May 4, 1961. D. T. Williams. August 1963. (PB-168223)

No. 19 Measurements by Aircraft of Condensed Water in Great Plains Thunderstorms. George P. Roys and Edwin Kessler. July 1966. (PB-173048)

No. 20 Field Operations of the National Severe Storms Project in Spring 1963. J. T. Lee, L. D. Sanders and D. T. Williams. January 1964. (PB-168224)

No. 21 On the Motion and Predictability of Convective Systems as Related to the Upper Winds in a Case of Small Turning of Wind with Height. James C. Fankhauser. January 1964. (PB-168225)

No. 22 Movement and Development Patterns of Convective Storms and Forecasting the Probability of Storm Passage at a Given Location. Chester W. Newton and James C. Fankhauser. January 1964. (PB-168226)

No. 23 Purposes and Programs of the National Severe Storms Laboratory, Norman, Oklahoma. Edwin Kessler. December 1964. (PB-166675)

No. 24 Papers on Weather Radar, Atmospheric Turbulence, Sferics, and Data Processing. August 1965. (AD-621586)

No. 25 A Comparison of Kinematically Computed Precipitation with Observed Convective Rainfall. James C. Fankhauser. September 1965. (PB-168445).

No. 26 Probing Air Motion by Doppler Analysis of Radar Clear Air Returns. Roger M. Lhermitte. May 1966. (PB-170636)

No. 27 Statistical Properties of Radar Echo Patterns and the Radar Echo Process. Larry Armijo. May 1966. The Role of the Kutta-Joukowski Force in Cloud Systems with Circulation. J. L. Goldman. May 1966. (PB-170756)

No. 28 Movement and Predictablity of Radar Echoes. James Warren Wilson. November 1966. (PB-173972)

No. 29 Notes on Thunderstorm Motions, Heights, and Circulations. T. W. Harrold, W. T. Roach, and Kenneth E. Wilk. November 1966. (AD-644899)

No. 30 Turbulence in Clear Air Near Thunderstorms. Anne Burns, Terence W. Harrold, Jack Burnham, and Clifford S. Spavins. December 1966. (PB-173992)

No. 31 Study of a Left-Moving Thunderstorm of 23 April 1964. George R. Hammond. April 1967. (PB-174681)

No. 32 Thunderstorm Circulations and Turbulence from Aircraft and Radar Data. James C. Fankhauser and J. T. Lee. April 1967. (PB-174860)

No. 33 On the Continuity of Water Substance. Edwin Kessler. April 1967. (PB-175840)

No. 34 Note on the Probing Balloon Motion by Doppler Radar. Roger M. Lhermitte. July 1967. (PB-175930)

No. 35 A Theory for the Determination of Wind and Precipitation Velocities with Doppler Radars. Larry Armijo. August 1967. (PB-176376)

No. 36 A Preliminary Evaluation of the F-100 Rough Rider Turbulence Measurement System. U. O. Lappe. October 1967. (PB-177037)

No. 37 Preliminary Quantitative Analysis of Airborne Weather Radar. Lester P. Merritt. December 1967. (PB-177188)

No. 38 On the Source of Thunderstorm Rotation. Stanley L. Barnes. March 1968. (PB-178990)

No. 39 Thunderstorm - Environment Interactions Revealed by Chaff Trajectories in the Mid-Troposphere. James C. Fankhauser. June 1968. (PB-179659)

No. 40 Objective Detection and Correction of Errors in Radiosonde Data. Rex L. Inman. June 1968. (PB-180284)

No. 41 Structure and Movement of the Severe Thunderstorms of 3 April 1964 as Revealed from Radar and Surface Mesonetwork Data Analysis. Jess Charba and Yoshikazu Sasaki. October 1968. (PB-183310)

No. 42 A Rainfall Rate Sensor. Brian E. Morgan. November 1968. (PB-183979)

No. 43 Detection and Presentation of Severe Thunderstorms by Airborne and Ground-Based Radars: A Comparative Study. Kenneth E. Wilk, John K. Carter, and J. T. Dooley. February 1969. (PB-183572)

No. 44 A Study of a Severe Local Storm of 16 April 1967. George Thomas Haglund. May 1969. (PB-184-970)

No. 45 On the Relationship Between Horizontal Moisture Convergence and Convective Cloud Formation. Horace R. Hudson. March 1970. (PB-191720)

No. 46 Severe Thunderstorm Radar Echo Motion and Related Weather Events Hazardous to Aviation Operations. Peter A. Barclay and Kenneth E. Wilk. June 1970. (PB-192498)

No. 47 Evaluation of Roughness Lengths at the NSSL-WKY Meteorological Tower. Leslie D. Sanders and Allen H. Weber. August 1970. (PB-194587)

No. 48 Behavior of Winds in the Lowest 1500 ft in Central Oklahoma: June 1966 - May 1967. Kenneth C. Crawford and Horace R. Hudson. August 1970.

No. 49 Tornado Incidence Maps. Arnold Court. August 1970. (COM-71-00019)

No. 50 The Meteorologically Instrumented WKY-TV Tower Facility. John K. Carter. September 1970. (COM-71-00108)

No. 51 Papers on Operational Objective Analysis Schemes at the National Severe Storms Forecast Center. Rex L. Inman. November 1970. (COM-71-00136)

No. 52 The Exploration of Certain Features of Tornado Dynamics Using a Laboratory Model. Neil B. Ward. November 1970. (COM-71-00139)

No. 53 Rawinsonde Observation and Processing Techniques at the National Severe Storms Laboratory. Stanley L. Barnes, James H. Henderson and Robert J. Ketchum. April 1971.

No. 54 Model of Precipitation and Vertical Air Currents. Edwin Kessler and William C. Bumgarner. June 1971.

No. 55 The NSSL Surface Network and Observations of Hazardous Wind Gusts. Operations Staff. June 1971.

No. 56 Pilot Chaff Project at the National Severe Storms Laboratory. Edward A. Jessup. November 1971.

No. 57 Numerical Simulation of Convective Vortices. Robert P. Davies-Jones and Glenn T. Vickers. November 1971.

No. 58 The Thermal Structure of the Lowest Half Kilometer in Central Oklahoma: December 9, 1966 - May 31, 1967. R. Craig Goff and Horace R. Hudson. July 1972.

No. 59 Cloud-to-Ground Lightning Versus Radar Reflectivity in Oklahoma Thunderstorms. Gilbert D. Kinzer. September 1972.

☆ U.S. GOVERNMENT PRINTING OFFICE: 1972-784 208/1111 REGION NO. 8